Phenomenological modeling of electron-hole recombination in promising photo-catalytic magnetic materials

Nicholas J. Harmon[1, a)] and David Kumi[1, 1, b)]
Department of Physics and Engineering Science, Coastal Carolina University, Conway, SC 29526, USA

(Dated: 17 July 2024)

Recent experiments have demonstrated impressive photo-catalytic performances in spin-polarized materials. The existence of spin-dependent recombination between spin split bands has been suggested as the cause for at least part of the improved photo-catalysis. To test the efficacy of this mechanism, we develop a set of rate equations for carrier charge and spin to shed light on recent experiments with metal-defected or doped oxides, magnetically decorated metal-organic frameworks, and magnetically-doped perovskites. Our results show that recombination will be dependent on the band spin polarization and the lengthening of decay times can be optimized by engineering the electronic structure.

I. INTRODUCTION

In the past handful of years, a new branch of interest into photocatalysis has taken place wherein reaction efficiency is measured using inorganic magnetic catalysts. While spin-dependent reactions have been studied for some time[1–3] the work has been in the context of singlet-triplet transitions on which molecular reactions depend upon. The reactivity at the surface, which will not be the focus here, has been attributed to better photo-catalytic performance in recent years[4–7]. One other observation that has been used to explain the increased photo-catalysis is that optically generated carrier lifetimes are sometimes elongated by using a ferromagnetic catalyst and sometimes a magnetic field. These longer lifetimes allow for carriers to travel to the surface which increases carrier redox reactivity.[8] This Letter lays out a phenomenological theory to model generation and recombination in the ferromagnetic semiconducting catalysts that have demonstrated significant improvement in photocatalysis over non-magnetic catalysts. Present descriptions of spin-dependent recombination for photo-catalysts have been qualitative, vague, and sometime contradictory. Our work here will shed light on the important microscopics at play and moreover direct future experimental and theoretical research toward materials, such as half-metallic ferromagnets[9,10], that will achieve superior photo-catalytic yields.

A central observation correlated to the efficacy of ferromagnetic photo-catalysts has been the extension of photoluminescence (PL) lifetimes for ferromagnetic catalysts over their non-magnetic counterparts as first observed in metal-defected TiO_2 by Pan *et al.*[5]. This critical work led to further PL measurements by others in a variety of systems such as Fe_3O_4/n-TiO_2 nanoparticles[11], Mn-doped Co_3O_4[12], Co-doped Zn-based metal organic frameworks (MOFs)[13], and Mn or Fe-doped perovskite nanocrystals[14,15]. Another endeavor explored carrier lifetimes in Mn-doped perovskite nanoplates via reflectance measurements[16]. Gao *et al.* saw enhancements in photoelectrochemical performance using ferromagnetic $ZnFe_2O_4$ but did not perform any transient measurements of PL or reflectance. The longer fluorescence times has been accompanied by improved catalytic performance in some but not all[13,14] of the aforementioned experiments. Refs. 5 and 16 were able to correlate slower photo-carrier decay with increased H generation, pollutant degradation, and CO_2 reduction. Ref. 13 reports faster fluorescent decay alongside with CO_2 reduction for the more magnetic samples. Explanations for the the spin-dependent recombination in these articles are similar and Ref. 13 is representative when stating "*Under light irradiation, the spin-up electrons are excited to the LUMO (corresponds to the conduction band minimum), and the corresponding holes with the spin-up direction are left in the HOMO. The photoexcited spin-up elecrons will change their spin direction to spin down due to the spin-orbital coupling, hyperfine interaction, etc., while the spin-up holes remaining in the HOMO keep their spin direction. In this case, the charge recombination will be suppressed due to the spin mismatch of photoexcited electrons and holes, which illustrates that a high degree of spin polarization will bring about enhanced charge separation.*" Explanations such as this are qualitative and lack important details on how the density of states may control the spin relaxation and concomitant suppression of recombination. In fact, Ref. 13 finds shorter PL lifetimes in their magnetic MOF. In this Letter, a rate equation model is devised to encompass the various processes occurring during photoexcitation and recombination in magnetic semiconductors like those that have been studied in photocatalysis. Our model allows for a more detailed description of how charge lifetimes are enhanced and guides researchers on ways to further enhance those times.

II. RATE EQUATION MODEL

We begin by examining the density of states of an idealized ferromagnetic semiconductor in Fig. 1. Due to exchange interactions, in general, both the valence and conduction bands are split such that the density of states for up spins is different than the density of state for down spins. Fig. 1 (a) depicts 100% spin polarization at the top of the valence band but in most cases there will be both spin states leading to a polarization $|P_v| < 1$. Fig. 1 (a) shows an undoped sys-

a)Electronic mail: nharmon@coastal.edu
b)Electronic mail: dkumi@coastal.edu

tem where the Fermi level lies somewhere mid gap. In some of the ferromagnetic semiconductors demonstrating extended lifetimes[5,16], p-type behavior has been displayed so we will assume p-doping in our model here; extending to n-type is straightforward. Doping may be unintentional or a byproduct of producing the magnetic material (*e.g.* titanium vacancies in TiO_2[5] or doping with magnetic atoms such as Co or Mn). A consequence of doping is traps which leads to a non-radiative route for recombination and diminishes band-to-band recombination. These traps have been seen to capture valence electrons leading to equilibrium holes[17,18], with density p^0, which is shown in Fig. 1 (b).

For the exchange split density of states of the valence and conduction electrons, we write the following rate equations to encompass the effects of photo-excitation, spin relaxation, bimolecular electron-hole recombination, and electron capture by traps:

$$\frac{dp_\uparrow}{dt} = -\frac{\Gamma^v_{\uparrow-\downarrow}}{2}(p_\uparrow - p^0_\uparrow) + \frac{\Gamma^v_{\downarrow-\uparrow}}{2}(p_\downarrow - p^0_\downarrow) - k\left(p_\uparrow n_\uparrow - p^0_\uparrow n^0_\uparrow\right) \tag{1}$$

$$\frac{dp_\downarrow}{dt} = -\frac{\Gamma^v_{\downarrow-\uparrow}}{2}(p_\downarrow - p^0_\downarrow) + \frac{\Gamma^v_{\uparrow-\downarrow}}{2}(p_\uparrow - p^0_\uparrow) - k\left(p_\downarrow n_\downarrow - p^0_\downarrow n^0_\downarrow\right) \tag{2}$$

$$\frac{dn_\uparrow}{dt} = -\frac{\Gamma^c_{\uparrow-\downarrow}}{2}(n_\uparrow - n^0_\uparrow) + \frac{\Gamma^c_{\downarrow-\uparrow}}{2}(n_\downarrow - n^0_\downarrow) - k\left(n_\uparrow p_\uparrow - n^0_\uparrow p^0_\uparrow\right) - k_T(N_T - n_T)n_\uparrow \tag{3}$$

$$\frac{dn_\downarrow}{dt} = -\frac{\Gamma^c_{\downarrow-\uparrow}}{2}(n_\downarrow - n^0_\downarrow) + \frac{\Gamma^c_{\uparrow-\downarrow}}{2}(n_\uparrow - n^0_\uparrow) - k\left(n_\downarrow p_\downarrow - n^0_\downarrow p^0_\downarrow\right) - k_T(N_T - n_T)n_\downarrow \tag{4}$$

$$\frac{dn_T}{dt} = k_T(N_T - n_T)(n_\uparrow + n_\downarrow) \tag{5}$$

which are similar to previous modeling of photo-recombination in non-magnetic systems[17,18] except for the inclusion of the spin relaxation terms (Γ terms) and the exclusion of excitons. Γ^i_{j-k} are spin flip rates of carrier type $i \in \{\text{v(alence), c(onduction)}\}$ between subscripted spin states $j,k \in \{\uparrow,\downarrow\}$. k is the recombination coefficient for electrons and holes which we take to be spin independent. N_T is the total density of traps while n_T is the density of filled traps. p_i is the density of holes in the spin i valence band. n_i is the density of electrons in the spin i conduction band. Superscripted 0 for n and p are equilibrium values. Since a p-type material is assumed, $n^0_i = 0$. In general, there will be equilibrium hole states of both spin directions so the number density of holes in the up/down bands are $p^0_{\uparrow/\downarrow} = \frac{1\pm P_v}{2}p^0$.

Photoexcitation, at the bandgap energy (here shown to be the energy between spin up conduction and valence bands), will preferentially populate one spin in the conduction band over another as shown in Fig. 1 (c). Each number density of photoexcited electrons and holes is n_{ex} at $t = 0$. For simplicity we will assume that the distribution of spins in the conduction band at $t = 0$ mirrors that of the valence band so $\delta n_{\uparrow/\downarrow}(0) = n_{\uparrow/\downarrow}(0) = \frac{1\pm P_v}{2}n_{ex}$ where $\delta n_{\uparrow/\downarrow}$ is the non-equilibrium electron density. Similarly, $\delta p_{\uparrow/\downarrow}(0) = p_{\uparrow/\downarrow}(0) - p^0_{\uparrow/\downarrow} = \frac{1\pm P_v}{2}n_{ex}$.

After excitation, electron spins may relax between up and down states. Fig. 1 (c) shows the initially up polarized spins falling down in energy to the down states with rate $\Gamma^c_{\uparrow-\downarrow}$ due to spin interactions that may include spin-orbit and hyperfine effects. Similarly, hole spins also relax. Fig. 1 (d) illustrates electron spin relaxation back to the up states (expected to be much slower for the configuration shown), spin-dependent band recombination, and recombination through trapping centers. Without specifying the spin and charge states of the traps, we simplify their recombination by making their capture of electrons spin independent with rate k_T. The importance of asymmetric spin relaxation must be stressed. Conduction spins will populate down states at a higher amount than up states while holes are primarily present in the up valence band. This leads to a bottleneck where spin down electrons persist to much longer times than would be expected in a non-magnetic semiconductor[19,20].

Eqs. (1) are a set of nonlinear equations due to the $\delta n\delta p$ product terms that are formed from the $\delta n_i \delta p_i$ terms. As such, there are no closed-form expressions for the solutions. However, in the limit of low fluence or excitation densities such that $p^0 \gg n_{ex}$, $\delta n_i \delta p_i$ terms are negligibly small compared to $\delta n_i p^0_i$ terms. Likewise, since $\delta p_i \ll p^0$, p_i never stray far from their equilibrium values so we can completely neglect the dp_i/dt rate equations (the accuracy of this approximation is tested in Fig. 2). In addition, low fluence implies that trap filling is changed little from its equilibrium value of $n_T = p_0$ so $dn_T/dt \approx 0$ which leads to a set of two coupled linear first order differential equations:

$$\frac{d\delta n_\uparrow}{dt} = -\frac{\Gamma^c_{\uparrow-\downarrow}}{2}\delta n_\uparrow + \frac{\Gamma^c_{\downarrow-\uparrow}}{2}\delta n_\downarrow - kp^0_\uparrow \delta n_\uparrow - k_T(N_T - p_0)\delta n_\uparrow$$

$$\frac{d\delta n_\downarrow}{dt} = -\frac{\Gamma^c_{\downarrow-\uparrow}}{2}\delta n_\downarrow + \frac{\Gamma^c_{\uparrow-\downarrow}}{2}\delta n_\uparrow - kp^0_\downarrow \delta n_\downarrow - k_T(N_T - p_0)\delta n_\downarrow \tag{6}$$

which gives us a linear set of equation that we can solve. The full solutions for $\delta n_\downarrow$ and $\delta n_\uparrow$ can be found analytically but are too extensive to write. However the two non-zero eigenvalues (decay constants) of this set of equations are

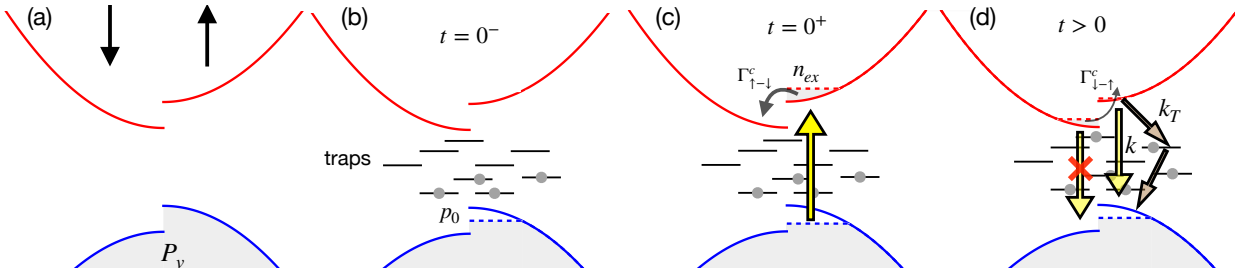

FIG. 1. Stages of electron-hole generation, spin population transfer, and recombination in a type II ferromagnetic semiconductor. (a) shows an ideal undoped half-metal ferromagnet. (b) traps are present in the material which we assume will collect valence electrons thereby introducing holes into the valence band. In our model, this represents our system just before photo-excitation. (c) Electrons and holes are excited upon illumination of an appropriate wavelength at which polarization is transferred into the conduction band. Due to the spin splitting, spin relaxation necessitates energy relaxation and up spins decrease and down spins increase in the conduction band. (d) photo-excited electrons may either (1) radiatively recombine with photo-excited or, more likely, doped holes at a rate k or (2) their spins may relax to the lower conduction band of opposite spin with rate $\Gamma^c_{\uparrow-\downarrow}$ or (3) non-radiatively leave the conduction band by being captured by traps, with capture coefficient k_T. At this later time, some now down spins from the population $n_{c,\downarrow}$ will relax back to the upper conduction band with rate $\Gamma^c_{\downarrow-\uparrow}$ but this process will be much slower due to the energetics. Radiative and non-radiative recombination will continue to deplete the spin up conduction band. Due to the spin selection rules, transitions from the spin down conduction band to the valence band will be weaker the larger P_{vb} is.

$$r_{fast/slow} = \frac{1}{4}(\Gamma^c_{\downarrow-\uparrow} + \Gamma^c_{\uparrow-\downarrow} + 2p^0 k + 4k_T(N_T - p^0)) \pm \frac{1}{4}\sqrt{(\Gamma^c_{\downarrow-\uparrow} - 2p^0 k P_v)^2 + 2(\Gamma^c_{\downarrow-\uparrow} + 2p^0 k P_v)\Gamma^c_{\uparrow-\downarrow} + \Gamma^c_{\uparrow-\downarrow}{}^2}. \quad (7)$$

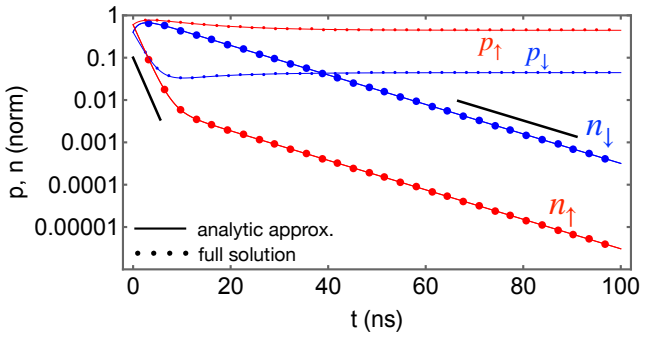

FIG. 2. Demonstration of agreement between analytical approximate solution and full numerical solution of rates equations for low fluence. The valence band density of states is split and the conduction band density of states are split as shown in Fig. 1. Black slope bars show rates $r_{fast/slow}$ from Eq. (7). Spin relaxation times are $1/\Gamma^c_{\uparrow-\downarrow} = 1$ ns, $1/\Gamma^c_{\downarrow-\uparrow} = 100$ ns, $1/\Gamma^v_{\downarrow-\uparrow} = 1$ ns, and $1/\Gamma^v_{\uparrow-\downarrow} = 10$ ns. Other parameters are $p^0 = 10^{15}$ cm^{-3}, $N_T = 5 \times 10^{15}$ cm^{-3}, $k = 10^{-7}$ cm^3/s, $k_T = 10^{-8}$ cm^3/s, $n_{ex} = 10^{13}$ cm^{-3}, and $P_v = 0.2$.

Figure 2 shows the validity of the analytic solution (solid lines) in the low fluence limit by comparing to the numerical solutions (circles) of the non-linear differential equations. Under the assumption of low fluence, the agreement between the two for conduction electron densities is extremely close. Non-equilibrium holes are tracked in the full solution but are ignored in the analytic. Due to the loss of electrons to traps, the photo-holes do not have recombinant partners so are thus retained at the longer times shown. In reality they will eventually recombine with trapped electrons on a longer timescale. While more up electrons are generated than down electrons, the up electrons rapidly relax into the down states whereas the vice versa process is much slower – this gives an abundance of down conduction spins.

III. MODELING SPIN-DEPENDENT RECOMBINATION IN FOR DIFFERENT CONFIGURATIONS OF DENSITY OF STATES

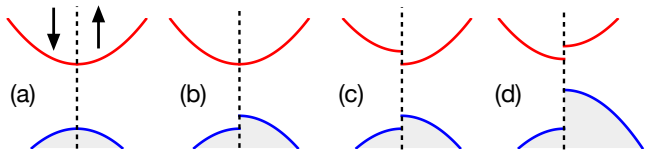

FIG. 3. Density of states schematics for (a) unpolarized bands (b) polarized valence band (c) Type I polarized conduction band (d) Type II polarized conduction band. Left (right) of the dashed line indicates down (up) states.

The rates found in Eq. (7) are dependent upon the spin flip rates, hole density, band polarization, and traps; we now seek out how these rates control carrier lifetimes for different densities of states arrangements. This knowledge will provide key insights into the design of materials for carrier lifetime optimization which is one factor controlling variable for photocatalysis. We now apply our linearized rate equation model to the four different scenarios schematized in Fig. 3.

- *(a) non magnetic.* When the density of states is equal for up and down spins, there is no spin-dependence in the generation and recombination so the loss of electronic carriers to either hole recombination or traps re-

duces to

$$r = \frac{1}{2} p_0 k + k_T (N_T - p_0) \tag{8}$$

where the first term is band-to-band recombination of electrons and doped holes.

- *(b) valence band splitting/no conduction band splitting.* When the density of states is equal for up and down conduction electrons, $\Gamma^c_{\uparrow-\downarrow} = \Gamma^c_{\downarrow-\uparrow} \equiv \Gamma^c$ which reduces $r_{fast/slow}$ to

$$r_{fast/slow} = \frac{1}{2}(\Gamma^c + p_0 k + 2k_T(N_T - p_0)) \tag{9}$$

$$\pm \frac{1}{2}\sqrt{(p_0 k P_v)^2 + \Gamma^{c2}} \tag{10}$$

which in the limits of very slow ($\Gamma^c \ll p_0 k P_v$) or very fast ($\Gamma^c \gg p_0 k P_v$) spin relaxation, becomes, respectively,

$$r_{fast/slow} = \frac{1}{2}(1 \pm P_v) k p_0 + k_T (N_T - p_0) \tag{11}$$

$$r_{fast/slow} = \Gamma_c/0 + \frac{k p_0}{2} + k_T (N_T - p_0) \tag{12}$$

where we see, for slow Γ^c, there is a polarization effect enhancing lifetime which competes with trapping. The solution is shown in Fig. 4 (a) for both $P_v = 0$ and 1 for intermediate situation where trapping and recombination time scales are comparable. For the polarized case, electrons are initiated up but quickly relax into the down states shown by the rapid rise of the blue curve at early times. Then trapping and band recombination lead to further decay. One observes a slight improvement in lifetime in the polarized case (*cf.* black and gray lines).

- *(c) type I conduction band splitting.* The conduction splitting implies $\Gamma^c_{\downarrow-\uparrow}$ much greater than $\Gamma^c_{\uparrow-\downarrow} \ll k p^0 P_v$, so $r_{fast/slow}$ becomes

$$r_{fast/slow} = \frac{1}{2}(1 \pm P_v) k p_0 + k_T (N_T - p_0) + 0/\frac{\Gamma^c_{\downarrow-\uparrow}}{2} \tag{13}$$

when $\Gamma^c_{\downarrow-\uparrow} < p_0 k P_v$ and

$$r_{fast/slow} = \frac{\Gamma^c_{\downarrow-\uparrow}}{2}/0 + \frac{1}{2}(1 \mp P_v) k p_0 + k_T (N_T - p_0) \tag{14}$$

when $\Gamma^c_{\downarrow-\uparrow} > p_0 k P_v$. The configuration is disadvantageous for photocatalysis as polarization leads to the overall more rapid decay shown in Fig. 4 (b). This is physically understood by noticing that excited up spin electrons are energetically unable to flip spins to the more 'protected' spin down states.

- *(d) type II conduction band splitting.* Under the conditions this alignment, $\Gamma^c_{\downarrow-\uparrow}$ much less than all other rates, $r_{fast/slow}$ reduces to

$$r_{fast/slow} = \frac{\Gamma^c_{\uparrow-\downarrow}}{2}/0 + \frac{1}{2}(1 \pm P_v) k p_0 + k_T (N_T - p_0). \tag{15}$$

Fig. 4 (c) shows a substantial increase in lifetime when polarization is at maximum. This is understood by generated up spins quickly flipping spins to down which have difficulty recombining with spin mismatched holes. Thus the lifetime is trap limited (*i.e.* decay rate for $P_v = 1$ is $k_T(N_T - p^0)$).

For the above calculations, we have attempted to use values that are comparable to what might be expected in the experiments of interest. We have ignored polaronic effects by using Langevin recombination theory to yield k values on the order of 10^{-7} cm^3/s[21–24]. Modeling by Peters *et al.* and Zhang *et al.* have found N_T in $CsPbBr_3$ on the order of a few 10^{14} cm^{-3}.[18,25] To conservatively analyze the polarization effects we have chosen a high number of traps 5×10^{15} cm^{-3} and $p^0 = 10^{15}$ cm^{-3} . By the same token, we choose a large k_T of 10^{-8} cm^3/s whereas in $CH_3NH_3PbI_{3-x}Cl_x$, k_T was determined to be 2×10^{-10} cm^3/s. We are unaware of any experimental or theoretical results for spin relaxation times in the magnetic systems we seek to understand. In halide perovskites spin relaxation times are on the order of picoseconds to nanoseconds depending on temperature.[26–28] We elect to utilize relaxation times in the nanosecond range. Choosing shorter times has little effect on the longer time dynamics of the carrier concentrations in Fig. 4.

Figure 5 displays the full r_{slow} as a function of trap filling (p^0 is being varied from 0 to N_T) for a type II DOS arrangement. The orange lines are when there are no traps so the equilibrium hole density is simply increasing. The rate increases as electrons find holes easier. Polarization decreases the rate since spin mismatching occurs more often leading to a bottleneck. The green curves show the rate when traps are present; there is a competition between rates as p^0 increases since electron-hole recombination increases but trap capture decreases as traps fill with valence electrons. Note that $\Gamma^c_{\downarrow-\uparrow}$ is not small enough for Eq. (15) to be valid.

IV. DISCUSSION

We now reexamine several of the experimental results on spin-dependent lifetimes with the insights gained from our rate equation model.

Guo *et al.* considered H_2O_2 in perovskite $Cs_3Cu_2Br_5$ nanocrystals that had been doped with magnetic Mn[15]. PL showed two exponential components – one lifetime was extended and one lifetime was diminished by the Mn. The long lived component was extended from 14.5901 μs to 56.797 μs which is the greatest enhancement in lifetimes in magnetic catalysts has have been reported. Guo *et al.* do not report

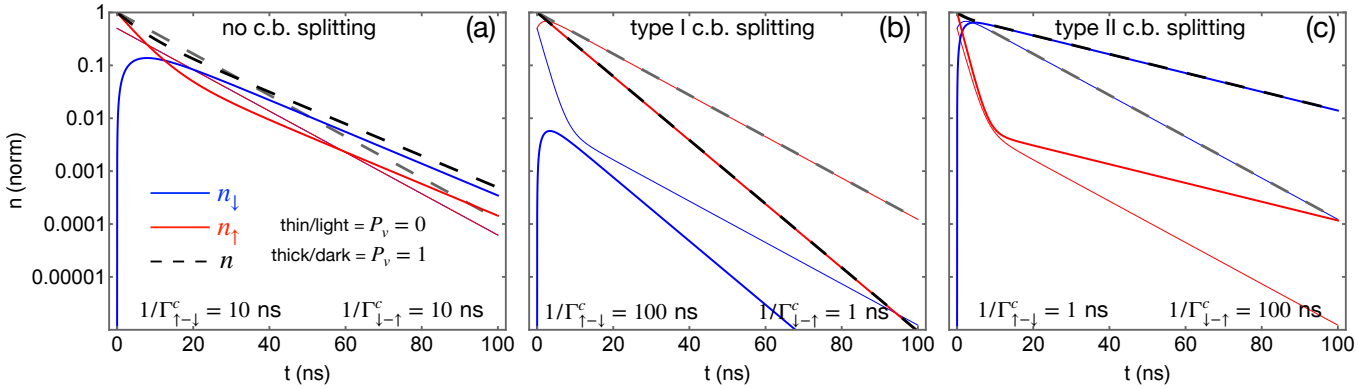

FIG. 4. Densities n, $n_\uparrow$, $n_\downarrow$ as functions of time for unpolarized (thin, lighter curves) and fully polarized (thick, darker curves) valence bands with each of the three different band offsets: (a) no conduction band splitting. For $P_v = 0$, $n_\uparrow$ and $n_\downarrow$ overlap. (b) type I conduction band splitting (c) type II conduction band splitting. Other parameters are $p_0 = 10^{15}$ cm^{-3}, $N_T = 5 \times 10^{15}$ cm^{-3}, $k = 10^{-7}$ cm^3/s, $k_T = 10^{-8}$ cm^3/s, and $n_{ex} = 10^{13}$ cm^{-3}. Curves are produced by the solutions Eqs. (6).

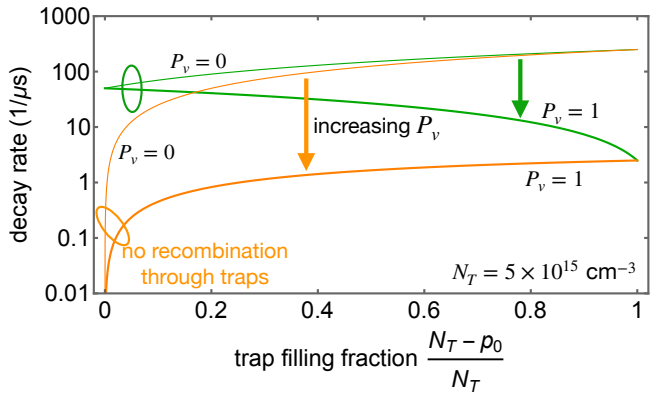

FIG. 5. Carrier decay rate, r_{slow} as a function of trap filling fraction. N_T is held constant and p_0 is varied from zero (filling fraction 0) to N_T (filling fraction 1). The two green curves are when traps capture electron and the orange curves neglect electron captures at trap sites. Thin curves show trends for unpolarized valence band. Thick curves show trends to maximally polarized valence band. relaxation times are $1/\Gamma^c_{\uparrow-\downarrow} = 1$ ns, $1/\Gamma^c_{\downarrow-\uparrow} = 100$ ns. Other parameters are $k = 10^{-7}$ cm^3/s, $k_T = 10^{-8}$ cm^3/s, and $n_{ex} = 10^{13}$ cm^{-3}.

any calculations of density of states so analyzing their data in terms of our model is not feasible. While Guo *et al.* speculate that the Mn dopants introducing traps as a cause for the fast decaying component, our model also suggests that spin polarization for type II density of states alignment introduces a fast decaying component as well.

Lin *et al.* also studied a perovskite material: Mn-doped $CsPbBr_3$ nanoplates[16] . A strong polarization dependence of reflectivity was observed and interpreted as proxy for carrier concentration. Their DFT calculations indicate the system being closer to at type II ferromagnet semiconductor with very little minority spin states in the conduction band. Of the two lifetimes observed, the longer lifetime increased by a factor of $\sim$2 when the host was doped with Mn. This large factor is consistent with our expectations for a type II system.

Kim *et al.* also examined $CsPbBr_3$ crystals but doped them with Fe[14]. The magnetic doping substantially decreased the two observed PL lifetimes (the longer of which reduced from 28.2 ns down to 5.9 ns). From their results, it is unclear how density of states is influenced by the the doping but in the doped system, the density of states is largely spin down over the energy range of the measured PL (near 2.5 eV or 500 nm); this would make the system type I so photoexcitations would be between conduction and valence bands of the same spin and spin relaxation would be largely ineffective at flipping spins into an anti-parallel bottleneck.

Y. Li *et al.* studied photocatalytic water splitting in nitrogen doped TiO_2 proximal to superparamagnetic Fe_3O_4 nanoparticles of systematically varying wieghts[11]. The authors also carried out various DFT calculations for the DOS and found that the superparamagnetic nanoparticle doping, in an applied magnetic field, led to spin polarized mid-gap states that induced strong valence band spin splitting. Since the conduction density of states is little affected by the magnetic field, the situation is nearest to Fig. 3(b) which suggests a longer PL lifetime in agreement with the observations of Y. Li *et al.* (monoexponential with lifetime 2.18 ns compared to biexponential with long lifetime 15.17 ns in sample with largest amount of Fe_3O_4)[11].

M. Li *et al.* explored photocatalytic CO_2 methanation when Mn was incorporated into Co_3O_4[12]. Their calculated DOS shows a type I arrangement with weak splitting of the conduction band. PL was measured to be dominated by a fast decay rate that was nearly independent of the Mn content. Less than 1% of the signal exhibited a Mn dependence by which the lifetime was enhanced by a factor of roughly two. The smallness of this polarization dependent contribution is suggestive of type I band alignment when $\Gamma^c_{\downarrow-\uparrow} < p_0 k P_v$ allows for some lifetime enhancement (see Eq. (13)) occurring for those electrons that are able to flip into a bottleneck.

Sun *et al.* examined three different Zn-based metal organic frameworks with varying degrees of magnetically split densities of states[13]. While CO_2 photo-reduction scaled positively with magnetic splitting, the fluorescent lifetimes showed a

slight decrease (0.369 ns down to 0.345 ns). Sun *et al.* DFT calculations for the three MOFs show that the most magnetic sample has much smaller valence splitting than conduction splitting. At the excitation energy of 3.43 eV (360 nm), most photo-excited electrons would occupy the lower spin conduction band which would be akin to the type I alignment of Fig. 3. Therefore the suppression of fluorescent lifetime is expected from our model. We speculate that the improved photocatalytic yield of CO is due some other possible spin-dependent aspect of the process.[4,5]

The results on anatase TiO_2 by Pan *et al.* are unique since the *p*-doping levels were varied and measured (1 - 5 $\times 10^{13}$ cm^{-3}) across the different defected samples. PL exhibited bi-exponential with the longest lifetime of 4.78 ns being present in the sample with the highest spin polarization. The pure TiO_2 was also bi-exponential with the longer lifetime being 4.10 ns. This rather weak dependence on doping indicates that electron-hole recombination is not the dominant pathway; due to the indirect band gap, the dominant recombinant pathway is likely non-radiative and through trapping sites – this is a linear-in-δn process of Eq. (6) that exists when few traps are filled (*i.e.* $N_T - p_0 \approx N_T$). This insensitivity to doping can be seen in Fig. 5 where in the low filling regime, the decay rates changes little (green curves).

A difficulty faced in all these experiments is that band magnetization cannot be controlled without changing other variables like defect or trap density and equilibrium holes. For example, when doping a semiconductor to induce magnetism, is the photocatalytic activity benefitting from the *p* doping (and accompanying mobility increase[29]) or the magnetism? Likewise, doping increases non-radiative recombination centers which affects photo-lifetimes. A handle that can be used to test the efficacy of spin dependent processes is the application of the magnetic field which many of the above experiments did utilize. As determined by Ref. 11, the affect of the field can still be complicated but it does not lead to additional trapping sites. Ref. 11 suggest the field acts on electron hole pairs through the Lorentz force as well as by magnetizing the magnetic nanoparticles. Another influence of the magnetic field would be on the spin precession of the photo-electrons which would alter their spin states and recombination dynamics.

V. CONCLUSIONS

Our model, though phenomenological and only semi-quantitative, points future experimental and theoretical/computational work in the following directions in order to understand and optimize magnetic photo-catalysts:

- band engineering is needed to create materials with optimal electronic structure in order to suppress recombination. To wit, strong splitting between up and down valence states allows for maximal optical generation of spin polarization into the conduction band. The conduction band should be split in same manner as shown in Figure 3 (d); this will allow for expedient spin flips into the optically inert minority spin state ($\downarrow$).

- theory will aide in finding optimum density of states for various materials but theory is also needed to investigate spin relaxation rates in these materials – especially how the spin flip rates depend on the band spin splitting.

- the role of mid-gap recombination centers warrants detailed experimental and theoretical investigation. These states will likely lead to spin-dependent capture[20,30] which could have repercussions on trap filling which in turn affects band recombination[31].

- as mentioned above, external magnetic fields are a probe that should be continued to be used to study spin-dependent photo-catalysis. As far as we can tell, the direction of the applied magnetic fields have not been reported. A field parallel versus perpendicular to the material's magnetization could lead to differing spin and recombination dynamics[32].

In light of our results, we hope to prompt the following directions to be taken to optimize and understand photocatalytic reactivity in magnetic materials:

- Technologically useful magnetic semiconductors have long been sought after[33,34] but have lacked high enough Curie temperatures. A decade ago TiO_2 was found to exhibit room temperature ferromagnetism[29] and since then other materials have as well. In what has been presented here, recombination suppression is dependent on the band polarization of the ferromagnet; half metals would be ideal materials to maximize the recombination bottleneck.[35,36] Half metals have recently been studied in double perovskites[9] and MOFs[10].

- The fact that photocatalytic performance is enhanced, whether carrier lifetimes are increased or decreased, suggests that carrier lifetimes are not the catalytic rate limiting step. Thus, in-depth examination of the spin-dependent processes of charge transport to the surface and surface reactivity are warranted.

To summarize, in this Letter we have presented a system of equations to describe electron-hole generation, spin relaxation, recombination and electron-trap recombination in the emerging field of magnetic dependent photo-catalysis. In the limit of monomolecular recombination, we derived decay rates for the photo-excited carriers. We investigated the role of band spin splitting on spin relaxation rates and put forth DOS configurations that will maximize carrier lifetimes. We find that recent experiments using magnetic semiconductors are consistent with our findings here. This work represents a first attempt at modeling the complex pathways involved in spin-dependent photocatalysis. Future extensions of the theory will be to incorporate exciton formation/dissociation, coherent spin evolution in magnetic fields, and study the role of fluence.

VI. ACKNOWLEDGEMENTS

NH was supported on this project by Coastal Carolina University through a PEG (Professional Enhancement Grant) and a FSRA (Faculty Summer Research Award).

VII. DATA AVAILABILITY

The data that support the findings of this study are available from the corresponding author upon reasonable request.

[1]H. J. Werner, Z. Schulten, and K. Schulten, "Theory of the magnetic field modulated geminate recombination of radical ion pairs in polar solvents: Application to the pyrene-n,n-dimenthylanline system," The Journal of Chemical Physics **67**, 646 (1977).
[2]K. Schulten and P. G. Wolynes, "Semiclassical description of electron spin motion in radicals including the effect of electron hopping," J. Chem. Phys. **68**, 3292 (1978).
[3]E. W. Knapp and K. Schulten, "Magnetic field. effect on the hyperfine-induced electron spin motion in radicals undergoing diamagnetic-paramagnetic exchange," J. Chem. Phys. **71**, 1878 (1979).
[4]W. Mtangi, F. Tassinari, K. Vankayala, A. Vargas Jentzsch, B. Adelizzi, A. R. A. Palmans, C. Fontanesi, E. W. Meijer, and R. Naaman, en"Control of Electrons' Spin Eliminates Hydrogen Peroxide Formation During Water Splitting," Journal of the American Chemical Society **139**, 2794–2798 (2017).
[5]L. Pan, M. Ai, C. Huang, L. Yin, X. Liu, R. Zhang, S. Wang, Z. Jiang, X. Zhang, J.-J. Zou, and W. Mi, en"Manipulating spin polarization of titanium dioxide for efficient photocatalysis," Nature Communications **11**, 418 (2020).
[6]F. A. Garcés-Pineda, M. Blasco-Ahicart, D. Nieto-Castro, N. López, and J. R. Galán-Mascarós, "Direct magnetic enhancement of electrocatalytic water oxidation in alkaline media," Nature Energy **4**, 519–525 (2019).
[7]T. Sun, Z. Tang, W. Zang, Z. Li, J. Li, Z. Li, L. Cao, J. S. Dominic Rodriguez, C. O. M. Mariano, H. Xu, *et al.*, "Ferromagnetic single-atom spin catalyst for boosting water splitting," Nature Nanotechnology **18**, 763–771 (2023).
[8]N. A. Deskins, P. M. Rao, and M. Dupuis, "Charge carrier management in semiconductors: modeling charge transport and recombination," in *Springer Handbook of Inorganic Photochemistry* (Springer, 2022) pp. 365–398.
[9]Q. Tang and X. Zhu, "Half-metallic double perovskite oxides: recent developments and future perspectives," Journal of Materials Chemistry C **10**, 15301–15338 (2022).
[10]X. Ni, H. Li, and J.-L. Brédas, "Half-Metallic Ferromagnetism in Radical-Bridged Metal–Organic Frameworks," Chemistry of Materials **36**, 2380–2389 (2024).
[11]Y. Li, Z. Wang, Y. Wang, A. Kovács, C. Foo, R. E. Dunin-Borkowski, Y. Lu, R. A. Taylor, C. Wu, and S. C. E. Tsang, "Local magnetic spin mismatch promoting photocatalytic overall water splitting with exceptional solar-to-hydrogen efficiency," Energy & Environmental Science **15**, 265–277 (2022).
[12]M. Li, S. Wu, D. Liu, Z. Ye, L. Wang, M. Kan, Z. Ye, M. Khan, and J. Zhang, "Engineering spatially adjacent redox sites with synergistic spin polarization effect to boost photocatalytic co2 methanation," Journal of the American Chemical Society (2024).
[13]K. Sun, Y. Huang, Q. Wang, W. Zhao, X. Zheng, J. Jiang, and H.-L. Jiang, "Manipulating the Spin State of Co Sites in Metal–Organic Frameworks for Boosting CO_2 Photoreduction," Journal of the American Chemical Society **146**, 3241–3249 (2024).
[14]T. H. Kim, K. Cho, S. H. Lee, J. H. Kang, H. B. Park, J. Park, and Y.-H. Kim, "Spin polarization in Fe-doped CsPbBr3 perovskite nanocrystals for enhancing photocatalytic CO2 reduction," Chemical Engineering Journal **492** (152095), 10.1016/j.cej.2024.152095.
[15]M. Guo, A. Talebian-Kiakalaieh, E. M. Hashem, B. Xia, J. Ran, and S.-Z. Qiao, "Magnetic mn-incorporated cs3cu2br5 nanocrystals for spin-polarized enhanced photocatalytic biomass conversion coupled with h2o2 evolution," Advanced Functional Materials , 2406356.
[16]C.-C. Lin, T.-R. Liu, S.-R. Lin, K. M. Boopathi, C.-H. Chiang, W.-Y. Tzeng, W.-H. C. Chien, H.-S. Hsu, C.-W. Luo, H.-Y. Tsai, H.-A. Chen, P.-C. Kuo, J. Shiue, J.-W. Chiou, W.-F. Pong, C.-C. Chen, and C.-W. Chen, "Spin-Polarized Photocatalytic CO_2 Reduction of Mn-Doped Perovskite Nanoplates," Journal of the American Chemical Society **144**, 15718–15726 (2022).
[17]S. D. Stranks, V. M. Burlakov, T. Leijtens, J. M. Ball, A. Goriely, and H. J. Snaith, "Recombination kinetics in organic-inorganic perovskites: excitons, free charge, and subgap states," Physical Review Applied **2**, 034007 (2014).
[18]J. A. Peters, Z. Liu, R. Yu, K. M. McCall, Y. He, M. G. Kanatzidis, and B. W. Wessels, "Carrier recombination mechanism in $CsPbBr_3$ revealed by time-resolved photoluminescence spectroscopy," Phys. Rev. B **100**, 235305 (2019).
[19]B. Jonker, L. Fu, W. Yu, W.-C. Chou, A. Petrou, and J. Warnock, "Long hole spin relaxation times in diluted magnetic semiconductor heterostructures," Journal of electronic materials **22**, 489–495 (1993).
[20]N. Lebedeva and P. Kuivalainen, "Modeling of ferromagnetic semiconductor devices for spintronics," Journal of Applied Physics **93**, 9845–9864 (2003).
[21]G. Samsonov, *The oxide handbook*.
[22]C. Wehrenfennig, G. E. Eperon, M. B. Johnston, H. J. Snaith, and L. M. Herz, "High charge carrier mobilities and lifetimes in organolead trihalide perovskites," Advanced Materials (Deerfield Beach, Fla.) **26**, 1584 (2014).
[23]D. W. Dequilettes, K. Frohna, D. Emin, T. Kirchartz, V. Bulovic, D. S. Ginger, and S. D. Stranks, "Charge-carrier recombination in halide perovskites: Focus review," Chemical reviews **119**, 11007–11019 (2019).
[24]J.-X. Song, X.-X. Yin, Z.-F. Li, and Y.-W. Li, "Low-temperature-processed metal oxide electron transport layers for efficient planar perovskite solar cells," Rare Metals **40**, 2730–2746 (2021).
[25]M. Zhang, Z. Zheng, Q. Fu, P. Guo, S. Zhang, C. Chen, H. Chen, M. Wang, W. Luo, and Y. Tian, "Determination of defect levels in melt-grown all-inorganic perovskite cspbbr3 crystals by thermally stimulated current spectra," The Journal of Physical Chemistry C **122**, 10309–10315 (2018).
[26]M. Zhou, J. S. Sarmiento, C. Fei, X. Zhang, and H. Wang, "Effect of composition on the spin relaxation of lead halide perovskites," The journal of physical chemistry letters **11**, 1502–1507 (2020).
[27]J. Xu, K. Li, U. N. Huynh, M. Fadel, J. Huang, R. Sundararaman, V. Vardeny, and Y. Ping, "How spin relaxes and dephases in bulk halide perovskites," Nature Communications **15**, 188 (2024).
[28]E. Kirstein, E. A. Zhukov, D. R. Yakovlev, N. E. Kopteva, E. Yalcin, I. A. Akimov, O. Hordiichuk, D. N. Dirin, M. V. Kovalenko, and M. Bayer, "Coherent carrier spin dynamics in fapbbr3 perovskite crystals," The Journal of Physical Chemistry Letters **15**, 2893–2903 (2024).
[29]S. Wang, L. Pan, J.-J. Song, W. Mi, J.-J. Zou, L. Wang, and X. Zhang, "Titanium-defected undoped anatase tio2 with p-type conductivity, room-temperature ferromagnetism, and remarkable photocatalytic performance," Journal of the American Chemical Society **137**, 2975–2983 (2015).
[30]N. J. Harmon, J. P. Ashton, P. M. Lenahan, and M. E. Flatté, "Spin-dependent capture mechanism for magnetic field effects on interface recombination current in semiconductor devices," Applied physics letters **123** (2023).
[31]E. Ivchenko, V. Kalevich, A. Y. Shiryaev, M. Afanasiev, and Y. Masumoto, "Optical orientation and spin-dependent recombination in gaasn alloys under continuous-wave pumping," Journal of Physics: Condensed Matter **22**, 465804 (2010).
[32]J. Qi, Y. Xu, N. Tolk, X. Liu, J. Furdyna, and I. Perakis, "Coherent magnetization precession in gamnas induced by ultrafast optical excitation," Applied Physics Letters **91** (2007).
[33]H. Tashpour and M. Vesaghi, "Spin dependent recombination in magnetic semiconductor," Applied Physics Letters **94** (2009).
[34]T. Dietl, "A ten-year perspective on dilute magnetic semiconductors and oxides," Nature materials **9**, 965–974 (2010).
[35]T. Kise, T. Ogasawara, M. Ashida, Y. Tomioka, Y. Tokura, and M. Kuwata-Gonokami, "Ultrafast spin dynamics and critical behavior in half-metallic ferromagnet: Sr 2 femoo 6," Physical Review Letters **85**, 1986 (2000).
[36]G. M. Müller, J. Walowski, M. Djordjevic, G.-X. Miao, A. Gupta, A. V. Ramos, K. Gehrke, V. Moshnyaga, K. Samwer, J. Schmalhorst, A. Thomas, A. Hütten, G. Reiss, J. S. Moodera, and M. Münzenberg, "Spin polarization

in half-metals probed by femtosecond spin excitation," Nature Materials **8**, 56–61 (2009).